

Modeling the Delayed Nonlinear Fiber Response in Ultra-Wideband Transmission Systems

Daniel Semrau

(¹) Infinera Corp., San Jose, CA, United States, dsemrau@infinera.com

Abstract For transmission beyond the C-band, the nonlinear fiber response cannot be considered instantaneous and its delayed contribution, the Raman response, needs to be included. Numerical and analytical modeling approaches are discussed and the impact of the complex-valued Raman spectrum on the nonlinear interference is shown.

Introduction

The delayed contribution of the nonlinear fiber response is given by the Raman response whose Fourier transform is the complex-valued Raman spectrum^{[1]-[3]}. Its imaginary part, that leads to inter-channel stimulated Raman scattering (ISRS), was recently included in numerical and analytical models in order to model ultra-wideband transmission systems^{[4]-[13]}. However, these approaches do not account for the real Raman spectrum and only indirectly include ISRS through artificially introduced loss profiles, neglecting temporal gain dynamics and complex interactions between various propagation effects.

In this paper, the modelling of the delayed nonlinear response is reviewed. Additionally, we present a highly accurate numerical model and an analytical closed-form model that is suitable for real-time computations.

Delayed fiber nonlinearity

To model delayed fiber nonlinearity, we introduced the generalized Manakov equation^[14] as

$$\begin{aligned} \frac{\partial}{\partial z} E_x = & \left(-\frac{\alpha}{2} - j\frac{\beta_2}{2} \frac{\partial^2}{\partial t^2} + \frac{\beta_3}{6} \frac{\partial^3}{\partial t^3} \right) E_x \\ & + j\gamma E_x \int h(\tau) \left[|E_x(z, t - \tau)|^2 + |E_y(z, t - \tau)|^2 \right] \end{aligned} \quad (1)$$

with the field envelopes $E_x(z, t)$ and $E_y(z, t)$ in x and y-polarizations, the attenuation coefficient α , the group velocity dispersion (GVD) β_2 , the GVD slope β_3 , the nonlinearity coefficient γ and $h(t)$ is the nonlinear impulse response. For single polarisation, Eq. (1) resembles the generalized nonlinear Schrödinger eq.^[15]. The nonlinear response is given by $h(t) = \frac{\xi}{9} (1 - f_r) \delta(t) + f_r h_r(t)$, with the fractional contribution of the Raman response

f_r and the Raman response $h_r(t)$. The Fourier transform of the Raman response is the normalized, complex-valued Raman spectrum $H_r(f) = \mathcal{F}\{h_r(t)\} = \frac{\lambda_0}{4\pi f_r n_2} [\tilde{n}_r(f) + j\tilde{g}_r(f)]$. $\tilde{n}_r(f)$ and $\tilde{g}_r(f)$ are the real and imaginary Raman spectrum, respectively. λ_0 and n_2 are the reference wavelength and the nonlinear refractive index. The fractional contribution is $f_r = \frac{\lambda_0}{4\pi n_2} \tilde{n}_r(0) = 0.23$ for $n_2 = 2.1 \cdot 10^{-20} \text{ m}^2\text{W}^{-1}$, which means that 23% of the nonlinear response stems from the Raman response. It is assumed that the nonlinearity coefficient was obtained from short or polarization-maintaining fibers^[16]. Without the Raman response ($f_r = 0$), Eq. (1) yields the conventional Manakov equation. The real and imaginary Raman spectrum are coupled via the Kramers-Kronig relations and shown in Fig. 1)a) for a Corning SMF-28 ULL fiber after^[14]. The imaginary Raman spectrum is the Raman gain spectrum and is responsible for inter-channel stimulated Raman scattering.

Analytical modeling in closed-form

Before the introduction of Eq. (1), only the imaginary Raman spectrum could be modeled. Additionally, authors would typically solve the well-known Raman gain equations^[17], which model ISRS in the *power* domain, and insert the resulting signal power profile as a generic gain function in the conventional Manakov equation^{[4]-[13]}. However, this approach neglects temporal gain dynamics of ISRS, the real part Raman spectrum and any dynamical interactions in the *field* domain between attenuation, dispersion, Kerr nonlinearity and the Raman response. Eq. (1), on the other hand, captures all these effects but needs to be solved using the computationally complex split-step Fourier method.

Recently, the imaginary Raman spectrum (ISRS) has also been included into analytical

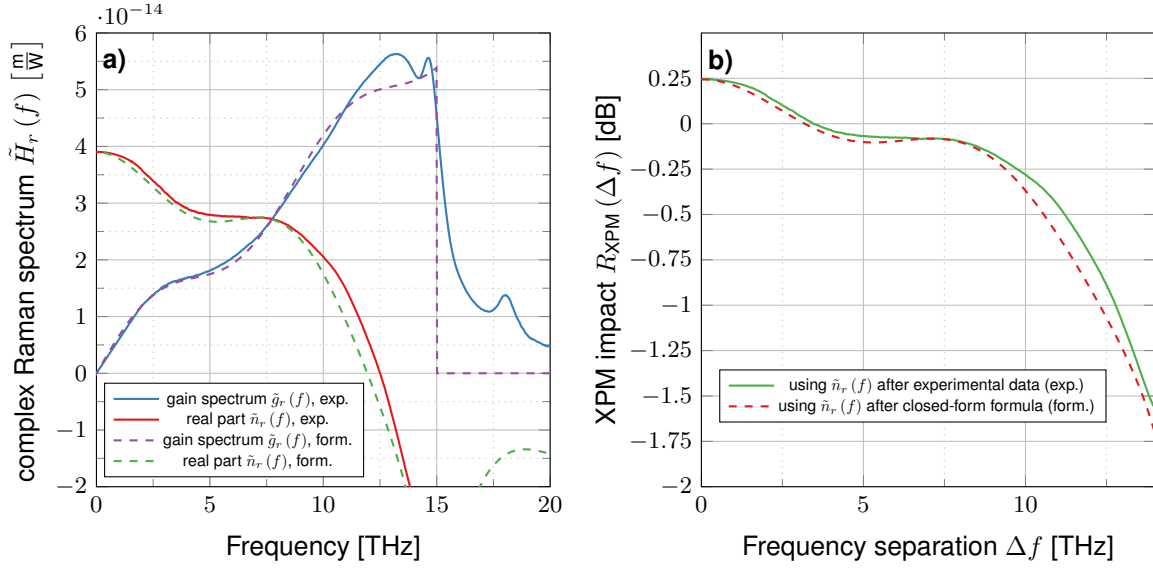


Fig. 1: Fig. a) shows the complex-valued Raman spectrum $\tilde{H}_r(f) = \tilde{n}_r(f) + j\tilde{g}_r(f)$ of a Corning[®] SMF-28[®] ULL fiber using experimental measurements (exp.) and formulas in closed-form (form.) after^[14]. Fig. b) shows the impact of the real Raman spectrum on the SPM/XPM contributions of the total NLI.

models, termed ISRS GN model, in integral-form^{[4]–[11]} and in closed-form for Gaussian modulation^{[12],[18]} and for arbitrary modulation formats^{[19],[20]}. All analytical approaches use a generic signal power profile obtained from the Raman gain equations^[17] to include ISRS. In^[14], we extended the ISRS GN model to include the real Raman spectrum to model the complete Raman response. In particular, we derived a simple closed-form formula for the functional shape of the real Raman spectrum as shown in Fig. 1a). More importantly, we analytically derived the impact of the real Raman spectrum on the SPM and XPM contributions of the total nonlinear interference (NLI). Only considering SPM and XPM contributions, the nonlinear SNR can be written as

$$\frac{P_{\text{ch}}^{-2}}{\text{SNR}_{\text{NLI}}} \approx R_{\text{SPM}}\eta_{\text{SPM}} + \sum_{\forall k} R_{\text{XPM}}(\Delta f)\eta_{\text{XPM}}^{(k)}, \quad (2)$$

with channel power P_{ch} , and the NLI coefficient η_{SPM} for SPM and $\eta_{\text{XPM}}^{(k)}$ being the XPM contribution from channel k onto the channel of interest with frequency separation Δf . The NLI coefficients can be obtained from the ISRS GN model in closed-form^{[18]–[20]}. $R_{\text{XPM}}(\Delta f)$ models the real Raman spectrum with $R_{\text{XPM}}(\Delta f) = R^2(\Delta f) + R(\Delta f)R(0) + R^2(0)$, $R(f) = \frac{9}{8\sqrt{3}}\Re\{H(f)\}$ and $R_{\text{SPM}} = R_{\text{XPM}}(0)$ ^[14].

The function $R_{\text{XPM}}(\Delta f)$ entirely describes the impact of the real Raman spectrum on the XPM contributions and is shown in Fig 2b) using the measured and modeled spectra in Fig. 1a). The increase of 0.25 dB at $\Delta f = 0$ originates from

the instantaneous component of the Raman response and the fact that the Raman response is not scaled by $\frac{8}{9}$ for dual-polarized signals^[16].

Using the ISRS GN model in closed-form^{[18]–[20]}, the spectrum formula in Fig. 1) (cf.^[14]) and Eq. (2) yields a model for the NLI entirely in closed-form, enabling real-time performance estimations. Hence, the reader has the choice between two options: high accuracy by numerically solving (1) or using the formalism in closed-form for results within microseconds while maintaining reasonable accuracy.

Results for C+L band transmission

In this section, the ISRS GN model in closed-form is used to estimate the nonlinear SNR in a network transmission scenario to compute the impact of the complex-valued Raman spectrum.

We assume a transmission window of 10 THz (entire C+L band), where the spectral channel occupancy is 30%. The channel location in frequency were sampled from an exponential distribution which is motivated by light path distributions that arise from k -shortest path - first fit (kSP-FF)^[21]. kSP-FF is a commonly used routing and wavelength assignment algorithm (RWA) that results in inhomogeneous channel slot occupation across the transmission window. The symbol rate was 5 Gbd and the launch power was -8 dBm which is approximately the optimum assuming EDFAs with 5 dB noise figure. The fiber parameters were $D = 16.4 \frac{\text{ps}}{\text{nm}\cdot\text{km}}$, $S = 0.067 \frac{\text{ps}}{\text{nm}^2\cdot\text{km}}$ and $\gamma = 1.04 \frac{1}{\text{W}\cdot\text{km}}$ with the Raman spectrum (form.) as shown in Fig. 1a). The transmission distance

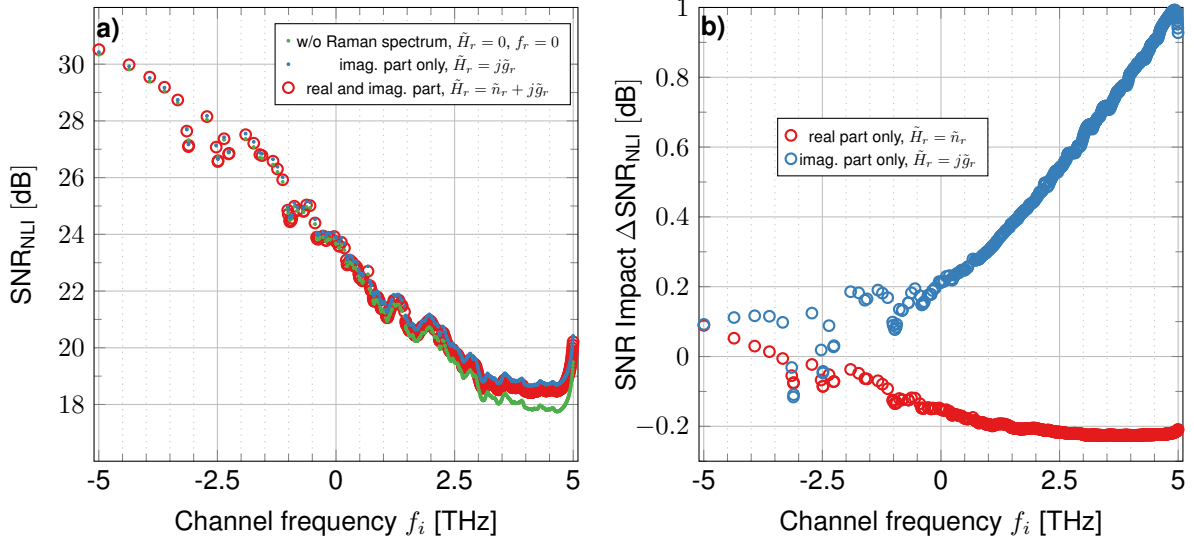


Fig. 2: Fig. a) shows the nonlinear SNR as a function of channel frequency for three cases: i) without the Raman spectrum, ii) including the imaginary part (ISRS) and iii) including the real and imaginary part. Fig. b) shows the individual impact of the real and imaginary Raman spectrum on the nonlinear SNR. All results were obtained using the ISRS GN model in closed-form.

was 10×80 km. The NLI coefficients as in (2) were estimated in closed-form from^[18]. Although the formulas in^{[18]–[20]} account for arbitrary modulation formats, a Gaussian modulation format is assumed, leading to conservative SNR estimates.

The nonlinear SNR as a function of channel frequency is shown in Fig. 2a) for three cases: First, without considering the Raman response ($f_r = 0$) which is not physical but this will serve as a baseline. The other two cases include the Raman response ($f_r \neq 0$). One case only includes the imaginary Raman spectrum (ISRS), while the other one includes the entire complex-valued Raman spectrum and hence the complete delayed nonlinear response. The impact of the real and imaginary Raman spectrum alone on the nonlinear SNR is shown in Fig. 2b).

The nonlinear SNR has a significant SNR tilt across the C+L band due to the inhomogeneous channel occupation. Channels at low frequencies have less closely spaced interferers and, due to dispersion, a higher nonlinear SNR as a consequence. For those channels most of the nonlinear interference stems from far spaced interferers. Fig. 2a) shows that including delayed fiber nonlinearity is not only the more accurate model, but it also improves the SNR for high frequency channels for the given spectral occupation.

The imaginary part (ISRS) depletes high frequency channels which in turn improves the SNR of those channels. On the contrary, ISRS amplifies low frequency channels which increases the SPM and XPM contributions of closely spaced channels. However, due to the inhomogeneous

channel occupation, most of the NLI of low frequency channels stems from high frequency channels that are depleted due to ISRS. For the imaginary part only, it seems that the SPM increase and the far spaced XPM reduction is somewhat balancing each other, resulting in an overall reduced ISRS impact at low frequencies. In fully occupied links, the impact of ISRS on the NLI is linear in decibel scale, with reduced nonlinear SNR at low frequencies^[5]. However, partially and inhomogeneously populated links behave differently due to far spaced XPM contributions.

Fig. 2b) shows that the real Raman spectrum introduces an additional NLI penalty of 0.25 dB at high frequencies. For those channels, the NLI is only scaled by $R_{\text{XPM}}(0)$ as far spaced XPM contributions are low (relatively) due to locally dense channel population. At low frequencies, the real Raman spectrum scales the XPM contributions according to Fig. 2b). The variation in terms of the total NLI (SNR) is around 0.3 dB with increased SNR at low frequencies due to the functional shape of $R_{\text{XPM}}(\Delta f)$.

Conclusion

We introduced the generalized Manakov equation and extended the ISRS GN model to numerically and analytically include the Raman response for accurate and very fast performance estimations of ultra-wideband transmission systems. Using a C+L band transmission example, the complex impact of the Raman response was shown with emphasis on spectral channel occupation and the relative NLI contributions between closely and far spaced interfering channels.

References

- [1] R. H. Stolen and E. P. Ippen, "Raman gain in glass optical waveguides", *App. Phys. Lett.*, vol. 22, no. 6, pp. 276–278, 1973.
- [2] R. H. Stolen, J. P. Gordon, W. J. Tomlinson, and H. A. Haus, "Raman response function of silica-core fibers", *J. Opt. Soc. Am. B*, vol. 6, pp. 1159–1166, 1989.
- [3] Q. Lin and G. P. Agrawal, "Raman response function for silica fibers", *Opt. Lett.*, vol. 31, pp. 3086–3088, 2006.
- [4] D. Semrau, R. Killey, and P. Bayvel, "Achievable rate degradation of ultra-wideband coherent fiber communication systems due to stimulated Raman scattering", *Opt. Express*, vol. 25, no. 12, pp. 13 024–13 034, Jun. 2017.
- [5] D. Semrau, R. I. Killey, and P. Bayvel, "The Gaussian Noise model in the presence of inter-channel stimulated Raman scattering", *J. Lightw. Technol.*, vol. 36, no. 14, pp. 3046–3055, Jul. 2018.
- [6] I. Roberts, J. M. Kahn, J. Harley, and D. W. Boertjes, "Channel power optimization of WDM systems following Gaussian noise nonlinearity model in presence of stimulated Raman scattering", *J. Lightw. Technol.*, vol. 35, no. 23, pp. 5237–5249, Dec. 2017.
- [7] M. Cantono, D. Pileri, A. Ferrari, C. Catanese, J. Thouras, J. L. Auge, and V. Curri, "On the interplay of nonlinear interference generation with stimulated Raman scattering for QoT estimation", *J. Lightw. Technol.*, pp. 1–1, Aug. 2018.
- [8] M. Cantono, J. L. Auge, and V. Curri, "Modelling the impact of SRS on NLI generation in commercial equipment: An experimental investigation", in *Optical Fiber Communication Conference*, Optical Society of America, 2018, p. M1D.2.
- [9] C. Lasagni, P. Serena, and A. Bononi, "A Raman-aware enhanced GN-model to estimate the modulation format dependence of the snr tilt in C+L band", in *European Conference on Optical Communication (ECOC)*, 2019.
- [10] C. Lasagni, P. Serena, and A. Bononi, "Modeling nonlinear interference with sparse Raman-tilt equalization", *J. Lightw. Technol.*, pp. 1–1, 2021.
- [11] H. Rabbani, G. Liga, V. Oliari, L. Beygi, E. Agrell, M. Karlsson, and A. Alvarado, "A general analytical model of nonlinear fiber propagation in the presence of Kerr nonlinearity and stimulated Raman scattering", *arXiv preprint arXiv:1909.08714*, 2019.
- [12] P. Poggiolini, M. Zefreh, G. Bosco, F. Forghieri, and S. Piciaccia, "Accurate non-linearity fully-closed-form formula based on the GN/EGN model and large-dataset fitting", in *Optical Fiber Communication Conference*, 2019.
- [13] P. Serena, C. Lasagni, S. Musetti, and A. Bononi, "On numerical simulations of ultra-wideband long-haul optical communication systems", *J. Lightw. Technol.*, vol. 38, no. 5, pp. 1019–1031, Sep. 2020.
- [14] D. Semrau, E. Sillekens, R. I. Killey, and P. Bayvel, "Modelling the delayed nonlinear fiber response in coherent optical communications", *J. Lightw. Technol.*, vol. 39, no. 7, pp. 1937–1952, 2021.
- [15] K. J. Blow and D. Wood, "Theoretical description of transient stimulated Raman scattering in optical fibers", *IEEE Journal of Quantum Electronics*, vol. 25, no. 12, pp. 2665–2673, Dec. 1989.
- [16] C. Antonelli, M. Shtaiif, and A. Mecozzi, "Modeling of nonlinear propagation in space-division multiplexed fiber-optic transmission", *J. Lightw. Technol.*, vol. 34, no. 1, pp. 36–54, Dec. 2016.
- [17] D. N. Christodoulides and R. B. Jander, "Evolution of stimulated Raman crosstalk in wavelength division multiplexed systems", *IEEE Photon. Technol. Lett.*, vol. 8, no. 12, pp. 1722–1724, Dec. 1996.
- [18] D. Semrau, R. I. Killey, and P. Bayvel, "A closed-form approximation of the Gaussian Noise model in the presence of inter-channel stimulated Raman scattering", *J. Lightw. Technol.*, pp. 1–1, Jan. 2019.
- [19] D. Semrau, E. Sillekens, R. I. Killey, and P. Bayvel, "A modulation format correction formula for the Gaussian Noise model in the presence of inter-channel stimulated Raman scattering", *J. Lightw. Technol.*, vol. 37, no. 19, pp. 5122–5131, Oct. 2019.
- [20] D. Semrau, L. Galdino, E. Sillekens, D. Lavery, R. I. Killey, and P. Bayvel, "Modulation format dependent, closed-form formula for estimating nonlinear interference in S+C+L band systems", in *European Conference on Optical Communication (ECOC)*, 2019.
- [21] R. J. Vincent, D. J. Ives, and S. J. Savory, "Scalable capacity estimation for nonlinear elastic all-optical core networks", *J. Lightw. Technol.*, vol. 37, no. 21, pp. 5380–5391, Nov. 2019.